Progress In Electromagnetics Research B, Vol. 11, 15–28, 2009

NEAR-FIELD RADIATION FROM COMMERCIAL CELLULAR PHONES USING A TEM CELL

N. Boriraksantikul, P. Kirawanich†, and N. E. Islam

Department of Electrical and Computer Engineering
University of Missouri-Columbia
Columbia, MO 65211, USA

Abstract—A technique to characterize the fields generated by a cell phone, and projected into an area inside a TEM cell for possible biological interaction studies is described. A double-ended monopole antenna is proposed as the lead signal inducer between the inside and the outside areas of the TEM cell. The coupling voltage at the TEM cell ports and the field distribution within the area under test (AUT) were found to be a function of the phone position, polarization, and dialing type. The measurements for a GSM 850 MHz cellular phone showed that the optimum setup is achievable when the phone is placed outside the TEM cell and co-polarized with the signal leader. An improvement of the field uniformity is possible with the use of a shorter signal leader but at the cost of decreased field strength. The proposed setup can be utilized in studies and experiments related to the radio frequency effects on biological cells and organs.

1. INTRODUCTION

With the proliferation of new high frequency electronic devices and gadgets in the marketplace there is an immediate concern about the risks to the general public regarding exposure to electromagnetic (EM) radiation. Studies of the biological effects of such radiation from these sources are an important emerging research topic. The potential use of cellular phones to cause brain tumors, cataracts, and aesthetic in humans have been reported [1–4].

Large test areas for measurements such as an anechoic chamber or large open space are not efficient when the area under exposure

† Also with the Department of Electrical Engineering, Mahidol University, Nakorn Pathom 73170, Thailand

is relatively small such as a biological sample. A TEM cell, on the other hand, which consists of a rectangular coaxial transmission section tapered with coaxial connectors on both ends is a better choice and offers a uniform EM field in a shielded environment. Effort to enhance its capabilities has been reported [5]. The usable area under test of the TEM cell is normally one-third of volume between the inner and outer conductors. It is widely used for radiated immunity and emission tests of electronic devices [5, 6], and its biological applications include SAR characterization [7], stress response on chromatin conformation in human lymphocytes [8].

TEM cells in their transverse mode operation cannot be used directly to simulate the effects of cellular phones on biological subjects. Effects of *in vitro* field exposure on the blood sample using a standard TEM cell and from a dipole that is equivalent to a mobile handset have produced different results [9]. Imaida et al. and Wang et al., in order to study the effects of *in vivo* near-field exposure on rodent brain and liver carcinogenesis, have used especially designed 'exposure boxes' to reproduce the cellular telephones [10, 11]. Another study to simulate a near-field EMI environment was reported by Das et al. where they fed the in-phase and out-of-phase signals into both ports of the TEM cell [12]. None of these efforts, however, utilized commercially available cellular phones as the sources of EM exposure.

In this paper, we report on a modified technique to use the TEM cell for conducting a radiated susceptibility test where a commercial cellular phone is the radiation source. Unlike conventional radiated susceptibility test, the TEM cell is driven by the cellular phone signals from outside, instead of the ports as described in [8] or as a near-field source replica [10, 11]. We propose a setup mechanism by attaching a double-ended monopole antenna on the top of the TEM cell's outer conductor as a signal leader, providing the near-field environment inside the TEM cell. Once the channel in the range of 800–915 MHz between the cellular phone and the base stations is established, the signals can propagate between the free space outside and inside the TEM cell through the signal leader. Our objective is to experimentally determine the optimum setup for the TEM cell that can be used as a near-field exposure box for radiation effects on biological cells. The consideration criteria are the coupling voltage obtained at the TEM cell ports and the field distribution within the usable area under test (AUT), where both of which are observed as functions of cellular phone position, polarization, and dialing type. Section 2 details the design of the TEM cell and its characterization. The experimental setup and results are discussed in Section 3. Finally, Section 4 provides the conclusion.

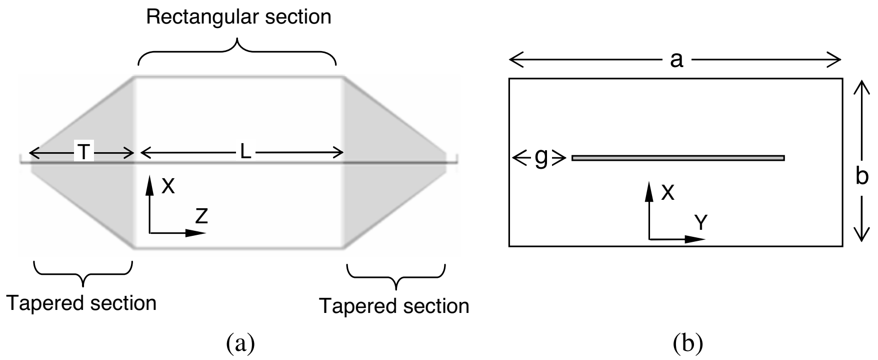

Figure 1. TEM cell configuration: (a) side view and (b) cross-sectional view. The parameters of the TEM cell dimension are $a = 50.4\,\text{cm}$, $b = 30.3\,\text{cm}$, $L = 50.4\,\text{cm}$, and $T = 27.6\,\text{cm}$.

2. TEM CELL DESIGN AND CHARACTERIZATION

The TEM cell in this work consists of a rectangular coaxial transmission section, which is tapered with the coaxial connectors on both ends, as shown in Fig. 1(a). The inner conductor, which is called the septum, acts as the positive conductor or the hot line. The outer conductor acts as the ground. The first key parameter to design is the impedance along the TEM cell. The equation of the impedance is given by [5, 6]

$$Z_o = \frac{1}{4\left[\frac{a}{b} - \frac{2}{\pi}\ln\left(\sinh\frac{\pi g}{2b}\right)\right] - \frac{\Delta C}{\varepsilon_o}}, \tag{1}$$

where a and b are the TEM cell's inner dimensions, and g is the gap between the septum and the outer conductor. Fig. 1(b) shows a cross-sectional view of the TEM cell's rectangular section with the parameters labeled. ΔC is the fringe capacitance between the edges of the center plate and the sidewalls of the TEM cell. If the ratio of a and b is larger than one, then we can ignore the term $\Delta C/\varepsilon_0$. With the desired impedance of 50 ohms, the relevant parameters a and b are 50.4 cm and 30.3 cm, respectively. The next parameter is the cutoff frequency of the TEM cell and it can be expressed as

$$f_c\left(TE_{mn}\right) = \frac{c}{2ab}\sqrt{b^2m^2 + a^2n^2}, \tag{2}$$

where c is the speed of light, and m and n represent the mode numbers. Since the dominant mode of the TEM cell is TE_{10}, which is the same as that of the rectangular waveguide, the first cutoff frequency of the TEM cell, therefore, is

$$f_c\left(TE_{10}\right) = \frac{c}{2a}. \tag{3}$$

The associated resonant frequency of the TEM cell is then given by

$$f_{res}\left(TE_{mnp}\right) = \sqrt{f_{cmn}^2 + \left(\frac{pc}{2l_{mn}}\right)^2} \tag{4}$$

where p is the mode number accounting for the reflections due to the tapered sections of the TEM cell, and l_{mn} is the resonant length of the TEM cell. The resonant frequency is basically used in determining the frequency range of the uniform field inside the TEM cell. The first term in the square root is the cutoff frequency where it can be calculated from (3), while the second term is associated with the resonant length of the TEM cell.

The TEM cell configuration in Fig. 1 is used in our simulations with the parameters $a = 50.4\,\text{cm}$, $b = 30.3\,\text{cm}$, $L = 50.4\,\text{cm}$, and $T = 27.6\,\text{cm}$. The full-wave simulations use CST Microwave Studio software based on the finite integral technique [13]. The material of the simulated TEM cell is perfect electric conductor (PEC). The TEM cell is designed in the horizontal direction, which means that the electric field vector is oriented in the x-direction, and the electromagnetic wave propagates along the z-direction. The simulated time domain reflectometer (TDR) result in Fig. 2(a) represents the characteristic impedance of the TEM cell, which is $50.84\,\Omega$. In addition, both peaks that appear in the TDR result correspond to the reflections at the TEM cell's ports. Fig. 2(b) shows the voltage standing wave ratio (VSWR) result where the value of 1.2 is monitored before the occurrences of the resonances. The result indicates that the first resonant frequency is 545 MHz, showing a good agreement with the value of 515.11 MHz calculated from analytical expression in (4).

3. EXPERIMENTAL SETUP AND RESULTS

The preliminary measurement in Fig. 3(a) was set up for verifying the laboratory constructed TEM cell with the results from previously discussed simulations. The results in Figs. 4(a) and 4(b) show, respectively, the impedance of 50.72 ohms and the first resonant frequency of 545 MHz by using a HP 8753D network analyzer. An approximately 0.2-ns difference of the second reflections in Figs. 2(a) and 4(a) is contributed from the difference between the dimension of

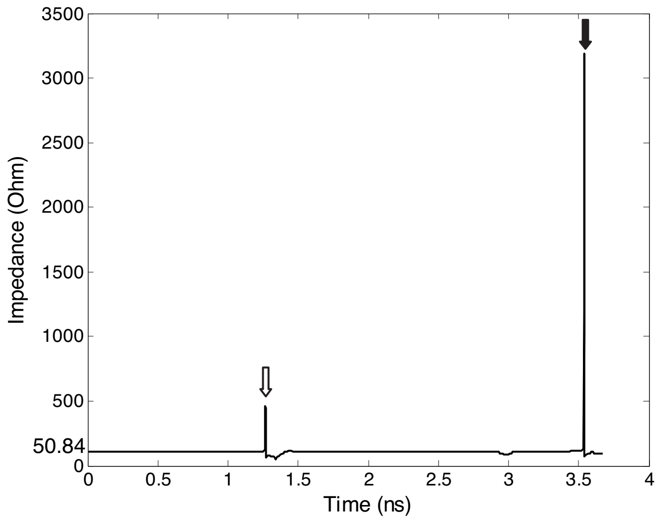

(a)

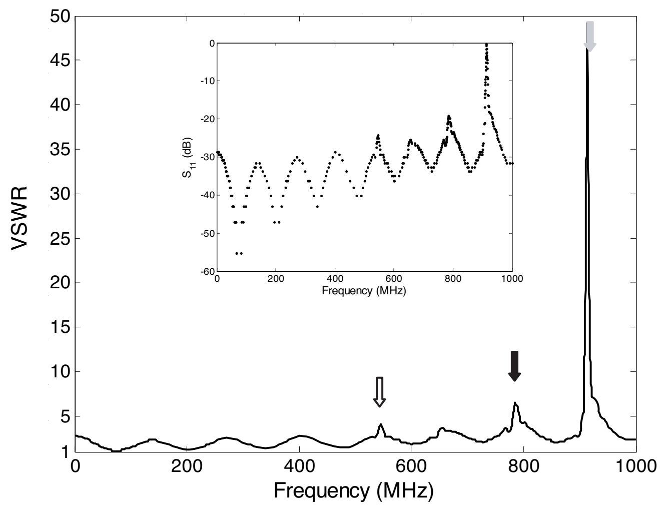

(b)

Figure 2. (a) The simulated time domain reflectometer (TDR) result with the resulting characteristic impedance of 50.84 Ω. (b) The voltage standing wave ratio (VSWR) result showing resonances. The inset is the associated S_{11} in dB.

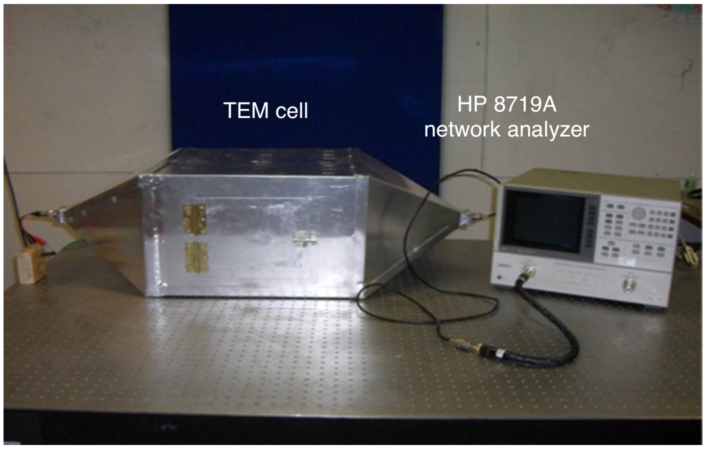

(a)

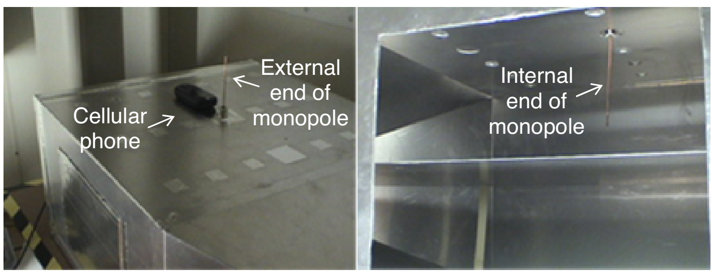

(b)

Figure 3. (a) Measurement setup for verifying the laboratory constructed TEM cell a HP 8753D network analyzer. (b) Setup for testing the cellular phone (AT&T Motorola C139) exposure.

the simulation model and the actual size of the TEM cell where the latter appears to be slightly smaller. The first two major resonances, as indicated by the arrows in Fig. 4(b), appear to match with the result in Fig. 2(b). The measured results confirm the TEM cell results from simulations. After validating the TEM cell, the next experiments were prepared for testing the exposure of the cellular phone (AT&T Motorola C139) where the setup is shown in Fig. 3(b) with a double-ended monopole antenna attached on the top of the TEM cell as a leading path of the cell phone signals between the TEM cell's interior and exterior. The length of the double-ended monopole ($h_1 + h_2$), where the detailed installation is shown in Fig. 5, was chosen in accordance with a half-wave length associated with

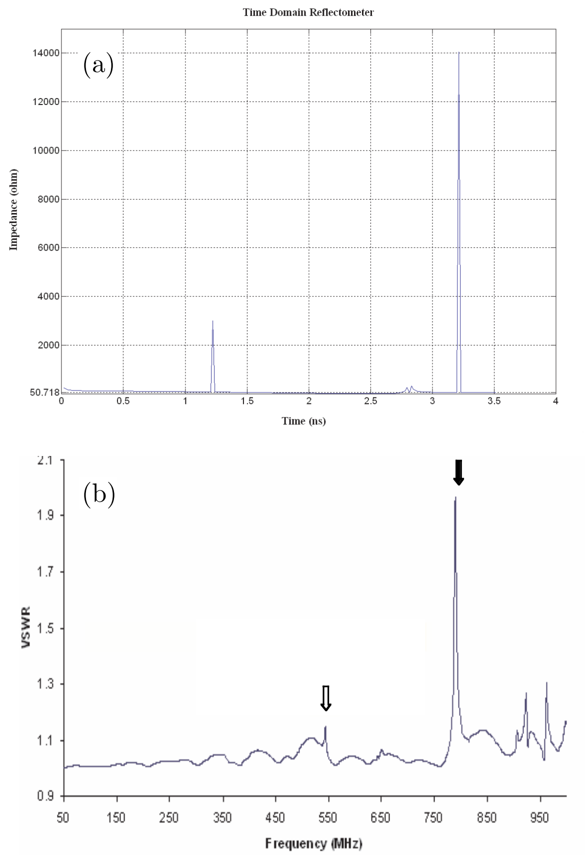

Figure 4. Measured results of (a) the time domain reflectometer (TDR) result with the resulting characteristic impedance of 50.72 Ω. (b) The voltage standing wave ratio (VSWR) result showing the major resonances indicated by the arrows.

the operating frequency of the cellular phone at 825.125 MHz for the optimum signal transceiving, i.e., receiving at the external monopole and transmitting at the internal monopole or vice versa. The simulated result of the TEM cell with the double-ended monopole installed is shown in Fig. 6(a). The influence of the monopole inclusion causes the second major resonant frequency [indicated by the black arrow] to shift higher to 800 MHz as compared to 786 MHz of the simulated result with the absence of the monopole in Fig. 2(b). The frequency shifting is due to the merging of two resonances in the same vicinity between the resonant frequency corresponding to the length of the monopole and

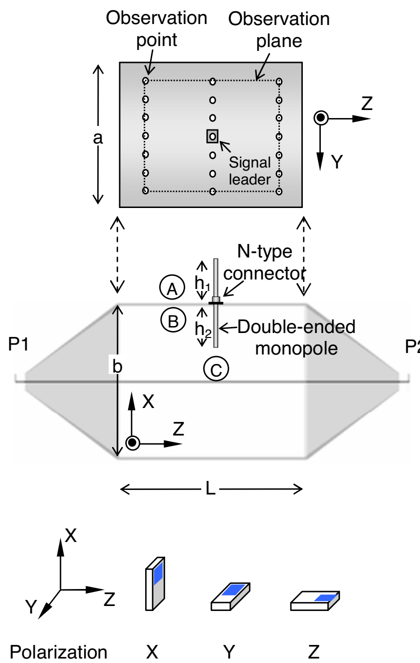

Figure 5. Experimental setup to monitor the field distribution inside the TEM cell and the details of the cellular phone polarization.

the resonant frequency of the TEM cell. The associated result from the measurement is shown in Fig. 6(b) where all resonant frequencies [indicated by the arrows] shift to the right compared with the simulated result in Fig. 6(a). This can be explained by the actual size of the TEM cell which seems to be smaller than that of the simulation model as mentioned previously.

The first experiment was designed to measure the coupling voltage amplitude at the TEM cell ports (P_1 and P_2) during establishing a call. The variables are the cellular phone polarization (X, Y, and Z), the location of the cellular phone, as indicated in Fig. 5, by labels A (external surface), B (internal surface), and C (on the septum), and the dialing type (in and out). The results, shown in Table 1, were obtained from 36 measurements. First, the results show that the highest coupling voltage occurs when the cellular phone is co-polarized with the signal leader in the x-axis. Secondly, the table indicates that there is no significant difference in coupling amplitude between dialing types. Finally, the results indicate that the coupling amplitude inside the TEM cell (locations B and C) is higher than outside (location A).

Table 1. 36 measurements of the coupling voltage amplitude at the TEM cell ports during cell phone calling at 825.125 MHz. The variables are the cell phone polarization, the cell phone location, and the dialing type.

Cell phone location	Voltage ($dB_{\mu}V$) with different cell phone polarizations (X,Y,Z)			
	Call in (825.125 MHz)		Call out (825.125 MHz)	
	Port 1	Port 2	Port 1	Port 2
A	93.74,76.16,79.57	92.39,76.23,81.07	93.51,74.14,79.57	91.36,75,81.41
B	101.5,87.68,88.48	98.73,86.25,92.93	98.81,76.32,87.34	96.53,78.7,83.52
C	99.98,90.1,90.56	99.74,91.32,90.86	99.9,90.47,90.2	100.2,90.46,90.99

This could be attributed to direct couplings between the cellular phone and the ports, and the effects of internal reflections introduced by the presence of cellular phone, which will have been further investigated in the next experiment. Note that the power level is independent of the call direction, but the distance to base station and obstacles. The results for call in and call out are very similar, and differences of the voltage levels are probably due to errors caused by the exact placement of the cellular phone and measurement inaccuracies.

The second experiment was designed to examine the field distribution within the AUT. An Agilent E7402A spectrum analyzer was used in association with the 9.4 cm antenna probe to monitor the electric field on the yz plane in the rectangular section. The field observation positions are arranged in a 7 by 3 matrix as shown in Fig. 5 through the top of the outer conductor plate. The center position was reserved for attaching the monopole. Fig. 7 shows the contour plots of the electric field distribution at 825.125 MHz on the observation plane with the testing cellular phone aligned in the x-axis, corresponding to the strongest coupling. The amplitudes of the fields are normalized by the field amplitude at the plane center. The measured profile in Fig. 7(a) is associated with the cellular phone at location A in accordance with calling-out signal. The similar distribution due to the calling-in signal is not shown here. The result suggests no significant difference in the field distribution between calling types. The comparison of the relative field distributions observed along the dashed-line indicated in Fig. 7(a) is shown in Fig. 7(b) as a function

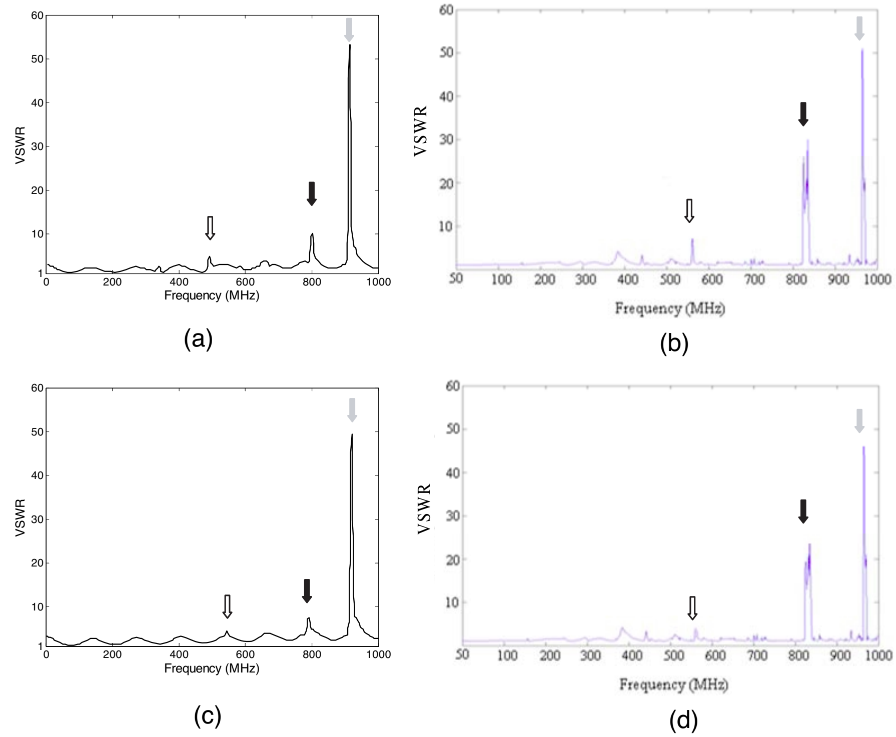

Figure 6. (a) Simulated VSWR result of the TEM cell with the 9-cm double-ended monopole and (b) the associated result from the measurement. (c) Simulated VSWR result of the TEM cell with the 1-cm double-ended monopole and (d) the associated result from the measurement. The arrows indicate the major resonances.

of cellular phone location (square = A, triangular = B, and circle = C). As expected, the field level is more uniform when the phone is establishing a call at location A. The configuration in Fig. 7(c) is the model for the simulation and the result of the field distribution in Fig. 7(d) provides a fair agreement with the measured result. It can also be noted from the profile shown in Figs. 7(a) that, even though the TEM cell is designed to have the monopole feed at the center for the TE_{10} mode excitation, the major contribution of the monopole's near-field radiation that is developed inside the TEM cell is from the TE_{30} excitation-mode due to the strong influence from the propagation-mode field inside the TEM cell. This can also be explained by the measured result of the VSWR using the monopole feed as shown in Fig. 6(b). The level of the VSWR at the frequency corresponding to the TE_{30}

cut-off frequency (black arrow) is higher than those at the TE_{10} cut-off frequency (white arrow).

An attempt was made to enhance the field uniformity by decreasing the length of the monopole as to reduce an obstacle size inside the TEM cell. By replacing the original monopole (9.4 cm) with the new monopole of 1-cm long, the suppression of the VSWR on the major resonances can be seen in Fig. 6(c) as compared to the result from using the original monopole in Fig. 6(a). The result of the associated measurement using the new monopole [see Fig. 6(d)] confirms the prediction from simulation. The relative VSWR of the 1 cm double-ended monopole referenced to the original monopole (9.4 cm) is shown in Fig. 8(a). The result suggests that the field fluctuation from the higher-order mode can be reduced as much as 4.3

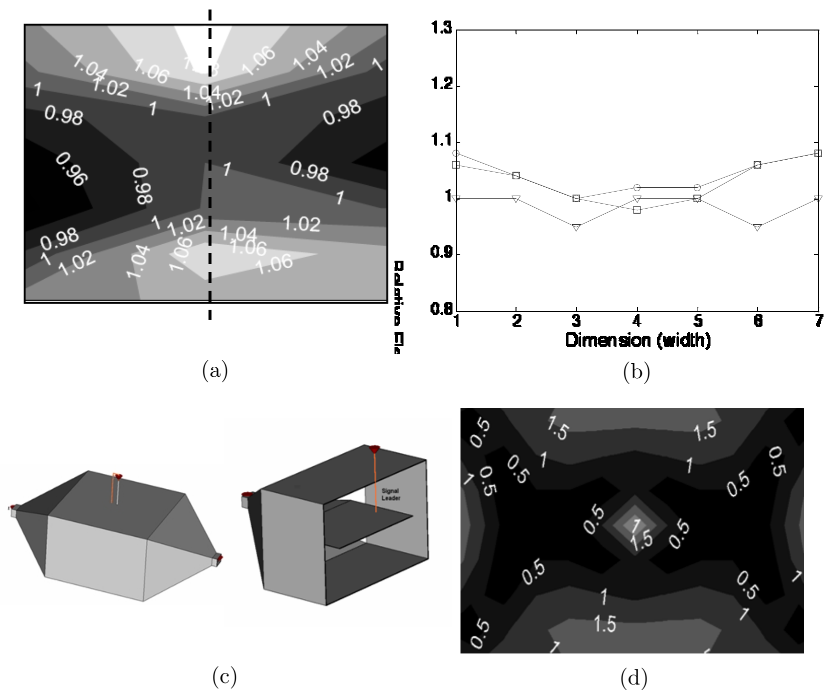

Figure 7. a) Measured profiles of the normalized electric field distribution at 825.125 MHz on the yz-plane during establishing with calling-out signal at location A. (b) Comparison of the field distribution level inside the TEM cell along the dashed-line indicated in figure 7(a) at different locations (square = A, triangular = B, and circle = C). (c) Simulation model of the TEM cell. (d) Associated simulation result of the field distribution.

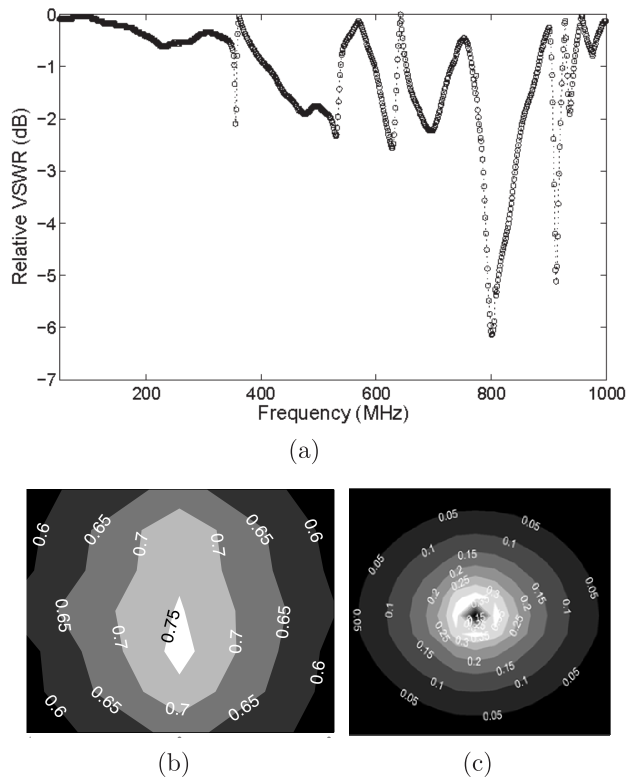

Figure 8. (a) Relative voltage standing wave ratio (VSWR) of the 1 cm monopole as referenced to the 9.4 cm signal monopole. (b) and (c) are the profiles of the normalized electric field distributions with the shorter monopole at 825.125 MHz from measurement and simulation, respectively.

decibels at 825.125 MHz with the shorter monopole. Fig. 8(b) is the profile of the electric fiels with the shorter monopole at 825.125 MHz. The field amplitude is normalized by the same factors used in Fig. 7. The profile shows more contributions from TE_{10p} fields, providing a closer environment to a near-field radiation from mobile headsets. Enhanced field uniformity suggests that a shorter signal leader can improve the size of the AUT but at the cost of decreasing the field strength. The associated result from simulation is shown in Fig. 8(c). A good agreement of the near-field distribution can be observed. The discrepancy of the field strength could be explained by a difference in length of the double-ended monopole used in the experiment and in the simulation.

4. CONCLUSION

This paper discusses an experiment design for electromagnetic radiation susceptibility and biological effects of electromagnetic radiation tests, using modified standard TEM cell and a commercial cellular phone as the excitation source. A double-ended monopole antenna is proposed as a signal leader to induce the cellular phone signals to propagate between the inner and outer regions of the TEM cell. The coupling voltage at the TEM cell ports and the field distribution within the area under test were observed as functions of cellular phone position, polarization, and dialing type. The measurements show that the optimum setup is when the cellular phone is placed outside the TEM cell and aligned in the same polarization with the signal leader. Further study on improvement of the field uniformity in the usable test area suggests the use of a shorter signal leader but at a cost of losing the field strength. Results suggest that this TEM cell setup can be applied to radio frequency exposure of the biological cells and organs for controlled experiments. Finally, since only one particular cellular phone was used in this study, the results will be different for experiments with other products due to antenna shape and parameters.

REFERENCES

1. Lin, J. C., "Specific Absorption Rates (SARs) induced in head tissues by microwave radiation from cell phones," *IEEE Antennas and Propagation Magazine*, Vol. 42, No. 5, Oct. 2000.
2. Lin, J. C., "Cell phone testing and fundamental scientific research," *IEEE Antennas and Propagation Magazine*, Vol. 43, No. 4, Aug. 2001.
3. Lin, J. C., "Can cell phones promote brain tumors: The interphone study?" *IEE Antennas and Propagation Magazine*, Vol. 47, No. 2, Apr. 2005.
4. Lin, J. C., "Health effects of cell-phone research outcomes and sources of funding," *IEEE Antennas and Propagation Magazine*, Vol. 49, No. 2, Apr. 2007.
5. Crawford, M. L., "Generation of standard EM fields using TEM transmission cells," *IEEE Trans. Electromagn. Compat.*, Vol. 16, Nov. 1974.
6. Crawford, M. L., J. L. Workman, and C. L. Thomas, "Expanding the bandwidth of TEM cells for EMC measurements," *IEEE Trans. Electromagn. Compat.*, Vol. 20, Nov. 1978.

7. Andrews, E. F., H. B. Lim, D. Xiao, S. Khamas, P. L. Starke, S. P. Ang, A. T. Barker, G. G. Cook, L. A. Coulton, and A. Scutt, "Investigation of SAR uniformity TEM cell exposed culture media," *IEEE Antenna Measurements and SAR*, 2004.
8. Sarimov, R., L. O. G. Malmgren, E. Markova, B. R. R. Persson, and I. Y. Belyaev, "Nonthermal GSM microwaves affect chromatin conformation in human lymphocytes similar to heat shock," *IEEE Trans. Plasma Sci.*, Vol. 32, No. 4, Aug. 2004.
9. Lim, H. B., G. G. Cook, A. T. Barker, and L. A. Coulton, "FDTD design of RF dosimetry apparatus to quantify the effects of near fields from mobile handsets on stress response mechanisms of human whole blood," *Int. J. Numer. Model.*, Vol. 15, 563–577, 2002.
10. Imaida, K., M. Taki, T. Yamaguchi, T. Ito, S. Watanabe, K. Wake, A. Aimoto, Y. Kamimura, N. Ito, and T. Shirai, "Lack of promoting effects of the electromagnetic near-field used for cellular phones (929.2 MHz) on rat liver carcinogenesis in a medium-term liver bioassay," *Carcinogenesis*, Vol. 19, 313–314, 1998.
11. Wang, J., M. Fujita, O. Fujiwara, K. Wake, and S. Watanabe, "Uncertainty evaluation of an in vivo near-field exposure setup for testing biological effects of cellular phones," *IEEE Trans. Electromagn. Compat.*, Vol. 48, No. 3, 545–551, Aug. 2006.
12. Das, S. K., V. Venkatesan, and B. K. Sinha, "A technique of electromagnetic interference measurements with high-impedance electric and low-impedance magnetic fields inside a TEM cell," *IEEE International Symposium on Electromagnetic Compatibility*, 367–369, Washington, DC, 1990.
13. CST MICROWAVE STUDIO Educational Version, CST Computer Simulation Technology, 2008.